

Attitude Dynamics and Control of a Nano-Satellite Orbiting Mars

Galen Savidge

University of Colorado at Boulder, Boulder, CO 80309

In this project we design and simulate an attitude control system for a nanosatellite in low Mars orbit. A simple two-satellite mission scenario is set up and then used to design a control system capable of tracking reference attitudes and autonomously switching between pointing modes. Expressions for attitude references and system dynamics are defined analytically. The uncontrolled and controlled system models are then simulated numerically.

I. Introduction

THERE is increasing interest among planetary science researchers in using nanosatellites to assist with communications or data collection on interplanetary missions. Let us construct an example of such a mission featuring two satellites in an orbit around Mars. The first, a nanosatellite in a low-Mars orbit, will be referred to as the "LMO spacecraft." The second is a larger "mother" satellite which will be named the "GMO spacecraft" after its geostationary Mars orbit. The LMO spacecraft is equipped with an array of sensors to take measurements of the Martian surface, a communications antenna to talk to the GMO spacecraft, and two flat solar arrays fixed such that they are co-planar. We will also assume that the LMO spacecraft has thrusters with sufficient torque capability for detumbling and three-axis attitude control.

The LMO spacecraft requires three pointing modes to be used in different phases of operation. The first is a science mode in which the sensor array is pointed towards nadir. Second is a communication mode, in which the antenna boresight must point at the GMO spacecraft. Last is a Sun-pointing mode, defined such that the Sun direction is normal to the solar array plane. Closed-loop attitude control is required to first detumble the satellite and then switch between these three modes throughout the lifetime of the mission. We will constrain the spacecraft to Sun-point when the Sun is visible, GMO-point when "near" the GMO spacecraft, and nadir point otherwise.

II. Problem Statement

We wish to simulate the attitude dynamics of the LMO spacecraft and design control laws to satisfy the required pointing modes. We will assume both spacecraft are in unperturbed (two-body) circular Mars orbits, with the initial orbital elements shown in Table 1. The LMO spacecraft has an inclined orbit with a 400 km altitude, while the GMO spacecraft follows an equatorial orbit with a period of one Mars day.

Table 1: Spacecraft Initial Mars-Centered Orbital Elements

Spacecraft	a	e	i	Ω	ω	Θ_0
LMO	3796.19 km	0	30°	20°	N/A	60°
GMO	20424.2 km	0	0°	0°	N/A	250°

A number of different references frames are required to solve this problem. First is the Mars-centered inertial frame N , defined such that \hat{n}_1 points at the Sun (we consider the Sun and Mars inertially fixed over the time range of interest) and \hat{n}_3 is normal to Mars' equatorial plane. Second is the LMO spacecraft body-fixed frame, or body frame, denoted B . This frame is defined such that the sensor platform is aligned with \hat{b}_1 , the communications antenna boresight points along $-\hat{b}_1$, and \hat{b}_3 is normal to the solar array plane. Next, each spacecraft has a local orbital (Hill) frame O , which is defined as follows: the \hat{i}_r unit vector is parallel to the spacecraft position vector \vec{r} ; the \hat{i}_h unit vector is parallel to the spacecraft angular momentum; and, the second unit vector \hat{i}_Θ completes the right hand rule, or more explicitly $\hat{i}_\Theta = \hat{i}_h \times \hat{i}_r$. The Hill frame of the LMO spacecraft is labelled H when it is necessary to differentiate

between it and the generalized orbit frame. We will also use a number of pointing reference frames, which will be denoted R and differentiated between by use of subscripts.

$$\begin{aligned}
N &= \{C_{Mars} : \hat{n}_1, \hat{n}_2, \hat{n}_3\} \\
B &= \{C_{m,LMO} : \hat{b}_1, \hat{b}_2, \hat{b}_3\} \\
O &= \{C_{m,S/C} : \hat{i}_r, \hat{i}_\Theta, \hat{i}_h\} \\
H &= \{C_{m,LMO} : \hat{i}_r, \hat{i}_\Theta, \hat{i}_h\} \\
R_* &= \{C_{m,LMO} : \hat{r}_1, \hat{r}_2, \hat{r}_3\}
\end{aligned} \tag{1}$$

We define the attitude state of the LMO spacecraft in terms the Modified Rodriguez Parameters (MRP) vector $\vec{\sigma}_{B/N}$ and the angular velocity vector $\vec{\omega}_{B/N}$. These vectors represent the attitude of the spacecraft body frame with respect to the inertial frame, and the angular velocity of the body frame with respect to the inertial frame. The initial attitude state of the spacecraft is defined for time t_0 in Eq. (2).

$$\vec{\sigma}_{B/N}(t_0) = \begin{bmatrix} 0.3 \\ -0.4 \\ 0.5 \end{bmatrix}, \quad {}^B\vec{\omega}_{B/N}(t_0) = \begin{bmatrix} 1.00 \\ 1.75 \\ -2.20 \end{bmatrix} \text{ deg/s} \tag{2}$$

When modelling the rotational dynamics of the LMO spacecraft, we will assume that the body frame axes are aligned with the body principle axes. The result is a diagonal body inertia matrix when expressed in body frame. The inertia of the LMO spacecraft is given in Eq. (3).

$${}^B[I]_{LMO} = \begin{bmatrix} 10 & 0 & 0 \\ 0 & 5 & 0 \\ 0 & 0 & 7.5 \end{bmatrix} \text{ kg m}^2 \tag{3}$$

III. Orbit Simulation

The first step in simulation of the circular orbits of this mission scenario is to derive an equation for the spacecraft position and linear velocity vectors \vec{r} and $\dot{\vec{r}}$. From the definition of the general orbit frame, $\vec{r} = r\hat{i}_r$, and $\vec{\omega}_{O/N} = \dot{\Theta}\hat{i}_\Theta$. Also note that in a circular orbit $\dot{\Theta} = \sqrt{\frac{\mu}{r^3}}$. Applying the transport theorem,

$$\dot{\vec{r}} = \frac{O}{dt}(\vec{r}) + \vec{\omega}_{O/N} \times \vec{r} = \vec{\omega}_{O/N} \times \vec{r} = r\dot{\Theta}\hat{i}_\Theta = r\sqrt{\frac{\mu}{r^3}}\hat{i}_\Theta = \sqrt{\frac{\mu}{r}}\hat{i}_\Theta \tag{4}$$

To find ${}^N\vec{r}$ and ${}^N\dot{\vec{r}}$ we can use Eqs. (5) & (6). The direction cosine matrix (DCM) $[ON]$ maps inertial vectors to Hill frame vectors and is constructed from the 3-1-3 Euler angle set (Ω, i, Θ) as shown in Eq. (7). Note we assume that the argument of periapsis is zero since the orbits of both spacecraft are circular.

$${}^O\vec{r} = \begin{bmatrix} r \\ 0 \\ 0 \end{bmatrix}, \quad {}^O\dot{\vec{r}} = \begin{bmatrix} 0 \\ \sqrt{\frac{\mu}{r}} \\ 0 \end{bmatrix} \tag{5}$$

$${}^N\vec{r} = [ON]{}^O\vec{r}, \quad {}^N\dot{\vec{r}} = [ON]{}^O\dot{\vec{r}} \tag{6}$$

$$[ON] = \begin{bmatrix} c[\Theta(t)]c(\Omega) - s[\Theta(t)]c(i)s(\Omega) & c[\Theta(t)]s(\Omega) + s[\Theta(t)]c(i)c(\Omega) & s[\Theta(t)](i) \\ -s[\Theta(t)]c(\Omega) - c[\Theta(t)]c(i)s(\Omega) & -s[\Theta(t)]s(\Omega) + c[\Theta(t)]c(i)c(\Omega) & c[\Theta(t)]s(i) \\ s(i)s(\Omega) & -s(i)c(\Omega)c(i) & \end{bmatrix} \tag{7}$$

IV. Orbit Frame Orientation

Recall that the Hill frame $H = \{\hat{i}_r, \hat{i}_\Theta, \hat{i}_h\}$ is defined as the orbit frame of the LMO spacecraft. We can find the orientation of this frame relative to the inertial frame using Eq. (7) and the spacecraft's known Keplerian elements. Since the orbit is circular,

$$\Theta_{LMO}(t) = \dot{\Theta}_{LMO} \cdot t + \Theta_{LMO,0} = \sqrt{\frac{\mu}{r_{LMO}^3}}t + \Theta_{LMO,0} \tag{8}$$

V. Sun-Pointing Reference Frame

We define the Sun-pointing reference frame $R_s = \{\hat{r}_1, \hat{r}_2, \hat{r}_3\}$ where \hat{r}_3 is aligned with the sun direction (\hat{n}_2) and \hat{r}_1 aligned with $-\hat{n}_1$. The third unit vector is given by the cross product of the first two. Note that this frame is fixed with respect to the inertial frame and thus $\vec{\omega}_{R_s/N} = \vec{0}$. The DCM $[R_s N]$ is constructed directly from the set of R_s unit vectors expressed in N .

$$\hat{r}_2 = \hat{r}_3 \times \hat{r}_1 = \hat{n}_2 \times -\hat{n}_1 = \hat{n}_3 \quad (9)$$

$$[R_s N] = \begin{bmatrix} {}^N \hat{r}_1^T \\ {}^N \hat{r}_2^T \\ {}^N \hat{r}_3^T \end{bmatrix} = \begin{bmatrix} -{}^N \hat{n}_1^T \\ {}^N \hat{n}_3^T \\ {}^N \hat{n}_2^T \end{bmatrix} = \begin{bmatrix} -1 & 0 & 0 \\ 0 & 0 & 1 \\ 0 & 1 & 0 \end{bmatrix} \quad (10)$$

We can verify that $[R_s N]^N \hat{n}_1^T = {}^{R_s} \hat{r}_2$, $[R_s]^N \hat{n}_1^T = -{}^{R_s} \hat{r}_1$, and $|[R_s N]| = 1$, meaning the matrix is a valid DCM and meets all of our stated requirements.

VI. Nadir Pointing Reference Frame

In nadir-pointing modes the spacecraft body vector \hat{b}_1 should be aligned with the nadir direction. Thus we will define the nadir pointing reference frame $R_n = \{\hat{r}_1, \hat{r}_2, \hat{r}_3\}$ such that $\hat{r}_1 = -\hat{i}_r$. We would also like \hat{b}_2 to be aligned with the velocity direction, meaning $\hat{r}_2 = \hat{i}_\Theta$. Then, $\hat{r}_3 = \hat{r}_1 \times \hat{r}_2 = -\hat{i}_h$, and we can proceed in a similar manner to before to find the DCM $[R_n H]$. The frame orientation with respect to the inertial frame can be found simply by post-multiplying by $[HN]$ (see Eq. (7)).

$$[R_n H] = \begin{bmatrix} {}^H \hat{r}_1^T \\ {}^H \hat{r}_2^T \\ {}^H \hat{r}_3^T \end{bmatrix} = \begin{bmatrix} -{}^H \hat{i}_r^T \\ {}^H \hat{i}_\Theta^T \\ {}^H \hat{i}_h^T \end{bmatrix} = \begin{bmatrix} -1 & 0 & 0 \\ 0 & 1 & 0 \\ 0 & 0 & -1 \end{bmatrix} \quad (11)$$

$$[R_n N] = [R_n H][HN] \quad (12)$$

The nadir pointing frame is fixed with respect to the Hill frame and thus their inertial angular velocities are equal. To find the angular velocity ${}^N \omega_{R_s/N}$ we can simply use the equivalent expression in H components.

$${}^N \vec{\omega}_{R_s/N} = {}^N \vec{\omega}_{H/N} = [HN]^T {}^H \vec{\omega}_{H/N} \quad (13)$$

For a circular orbit ${}^O \vec{\omega}_{O/N} = \sqrt{\frac{\mu}{r^3}} ({}^O \hat{i}_h)$, so

$${}^N \vec{\omega}_{R_s/N} = [HN]^T \cdot {}^H \begin{bmatrix} 0 \\ 0 \\ \sqrt{\frac{\mu}{r_{LMO}^3}} \end{bmatrix} \quad (14)$$

VII. GMO-Pointing Reference Frame

The final reference frame needed for the LMO spacecraft pointing modes is a GMO-spacecraft-pointing reference frame, which we will define as $R_n = \{\hat{r}_1, \hat{r}_2, \hat{r}_3\}$. In this frame the communication instruments of the spacecraft must be pointed towards the GMO spacecraft: $-\hat{b}_1$ must then be aligned with $\Delta \vec{r}$, where $\Delta \vec{r} = \vec{r}_{GMO} - \vec{r}_{LMO}$. The inertial positions of each spacecraft can be found using Eqs. (5) & (6). The second attitude constraint is given by

$$\hat{r}_2 = \frac{\Delta \vec{r} \times \hat{n}_2}{\|\Delta \vec{r} \times \hat{n}_2\|} \quad (15)$$

The third unit vector can be calculated using the cross product $\hat{r}_3 = \hat{r}_1 \times \hat{r}_2$. Inertial frame expressions of the \hat{r} unit vectors can again be used to calculate the DCM for the R_n frame.

$${}^N \hat{r}_1 = -{}^N \Delta \vec{r}, \quad {}^N \hat{r}_2 = \frac{{}^N \Delta \vec{r} \times {}^N \hat{n}_2}{\|{}^N \Delta \vec{r} \times {}^N \hat{n}_2\|}, \quad {}^N \hat{r}_3 = {}^N \hat{r}_1 \times {}^N \hat{r}_2 \quad (16)$$

$$[R_n N] = \begin{bmatrix} {}^N \hat{r}_1^T \\ {}^N \hat{r}_2^T \\ {}^N \hat{r}_3^T \end{bmatrix} \quad (17)$$

Calculating the relative motion between these two frames analytically is challenging. Instead, we will use numerical methods to estimate their relative angular velocity. We can start with the DCM differential kinematic equation, solve for the angular velocity vector $\vec{\omega}$, and then translate into inertial frame components. The DCM time derivative is estimated using a finite difference over a small time step. Since we expect spacecraft slews to last for a time period on the order of seconds, using $\delta t = 1\mu s$ should provide sufficient accuracy.

$$[\dot{R}_c N] \approx \frac{[R_c N](t_0 + \delta t) - [R_c N](t_0)}{\delta t} \quad (18)$$

$$[\dot{R}_c N] = -[\tilde{\omega}_{R_c/N}][R_c N] \quad \longrightarrow \quad -[\tilde{\omega}_{R_c/N}] = [\dot{R}_c N][R_c N]^T = [W] \quad (19)$$

We can now extract angular velocity components directly from $[W]$ by "inverting" the skew symmetric matrix operator. Due to assumptions made in the DCM differential kinematic equation, the angular velocity vector found this way will have components expressed in R_c and must be converted to inertial frame components as shown in Eq. (21).

$${}^{R_c}\vec{\omega}_{R_c/N} = {}^{R_c} \begin{bmatrix} W_{23} \\ W_{31} \\ W_{12} \end{bmatrix} \quad (20)$$

$${}^N\vec{\omega}_{R_c/N} = [R_c N]^T \cdot {}^{R_c}\vec{\omega}_{R_c/N} \quad (21)$$

VIII. Attitude Error Evaluation

Closed-loop attitude control requires the calculation of "errors" in both attitude and angular velocity. To do this we need both the relative attitude and relative velocity between the body frame B and one of the three reference frames, which we will call R . The reference frame attitude is given in DCM form, while the body attitude in the state vector is in MRP form. An attitude set conversion is required – we choose to use DCMs to find the relative attitude, then convert the result back to an MRP in the final step. Equations (22), (23), & (24) outline this process.

$$[BN] = [I_3] + \frac{8[\tilde{\sigma}_{B/N}]^2 - 4(1 - \sigma_{B/N}^2)[\tilde{\sigma}_{B/N}]}{(1 + \sigma_{B/N}^2)^2} \quad (22)$$

$$[BR] = [BN][RN]^T \quad (23)$$

$$\tilde{\sigma}_{B/R} = \frac{1}{\zeta(\zeta + 2)} \begin{bmatrix} BR_{23} - BR_{32} \\ BR_{31} - BR_{13} \\ BR_{12} - BR_{21} \end{bmatrix}, \quad \zeta = \sqrt{\text{tr}([BR]) + 1} \quad (24)$$

The relative angular velocity between B and R can be found by simply by calculating the vector difference between the frames' angular velocities with respect to a third frame, in this case the inertial frame. Note that the reference frame angular velocity is provided in inertial frame components and must be converted to body frame components.

$${}^B\vec{\omega}_{B/R} = {}^B\vec{\omega}_{B/N} - [BN]{}^N\vec{\omega}_{R/N} \quad (25)$$

IX. Numerical Attitude Simulator

Control algorithm testing requires accurate simulation of the attitude dynamics of the spacecraft. To this end we used a numerical integrator which solves the initial value problem posed by the spacecraft rotational equations of motion and initial state. Defining a six-element state vector as shown in Eq. (28), attitude and angular velocity can be forward integrated together using Runge-Kutta (RK4) methods. The first-order equations of motion for this system are given by Euler's equation of rotational motion Eq. (26) and the MRP differential kinematic equation Eq. (27), where \vec{L} is external torque around body center of mass.¹ The dynamics are shown in matrix form in Eq. (28).

$$[I]\dot{\vec{\omega}} = -[\tilde{\omega}][I]\vec{\omega} + \vec{L} \quad (26)$$

$$\dot{\vec{\sigma}} = \frac{1}{4}[(1 - \sigma^2)[I_3] + 2[\tilde{\sigma}] + 2\tilde{\sigma}\tilde{\sigma}^T]{}^B\vec{\omega} \quad (27)$$

$$\begin{aligned}
X &= \begin{bmatrix} \vec{\sigma}_{B/N} \\ {}^B\vec{\omega}_{B/N} \end{bmatrix} \\
\dot{X} &= \begin{bmatrix} \frac{1}{4}[(1 - \sigma_{B/N}^2)[I_3] + 2[\vec{\sigma}_{B/N}] + 2\vec{\sigma}_{B/N}\vec{\sigma}_{B/N}^T] {}^B\vec{\omega}_{B/N} \\ {}^B[I]^{-1}({}^B\vec{\omega}_{B/N})^B[I] {}^B\vec{\omega}_{B/N} + {}^B\vec{L} \end{bmatrix}
\end{aligned} \tag{28}$$

X. Attitude Control Law

We will use a simple PD controller for attitude control of the LMO spacecraft. The body attitude and angular velocity must track those of a reference frame, so the error quantities from Eqs. (24) & (25) can be used. Switching between pointing modes is then accomplished by changing which reference frame (R_s , R_n , or R_c) is calculated and passed into the controller.

$${}^B\vec{u} = -K\vec{\sigma}_{B/R} - P {}^B\vec{\omega}_{B/R} \tag{29}$$

Since the inertia matrix $[I]$ is diagonal and the gain matrices K and P are scalar, the linearized equations of motion can be decoupled as shown in Eq. (30).¹

$$\begin{bmatrix} \dot{\sigma}_i \\ \dot{\omega}_i \end{bmatrix} = \begin{bmatrix} 0 & \frac{1}{4}P \\ -\frac{K}{I_i} & -\frac{P}{I_i} \end{bmatrix} \begin{bmatrix} \sigma_i \\ \omega_i \end{bmatrix} \tag{30}$$

Finding the poles of the equation above leads to the following equations for the natural frequency, damping ratio, and decay time constant of each component:

$$\begin{aligned}
\omega_{n_i} &= \frac{1}{2I_i} \sqrt{KI_i} \\
\xi_i &= \frac{P}{\sqrt{KI_i}} \\
T_i &= \frac{2I_i}{P}
\end{aligned} \tag{31}$$

We choose the gains K and P such that (1) the highest decay time constant of the three is exactly 120 seconds, and (2) the highest damping ratio is exactly 1 (critically damped). Noting that the highest decay time corresponds to the axis of highest inertia, and the highest damping ratio corresponds to the axis of lowest inertia,

$$T_1 = \frac{2I_1}{P} = 120 \text{ s} \implies P = \frac{2I_1}{120 \text{ s}} = \frac{2 \times 10 \text{ kg m}^2}{120 \text{ s}} \implies P = \frac{1}{6} \text{ kg m}^2/\text{s} \tag{32}$$

$$\begin{aligned}
\xi_2 = \frac{P}{KI_2} = 1 &\implies P^2 = KI_2 \implies K = \frac{P^2}{I_2} = \frac{(\frac{1}{6} \text{ kg m}^2/\text{s})^2}{5 \text{ kg m}^2} \\
&\implies K = \frac{1}{180} \text{ kg m}^2/\text{s}^2
\end{aligned} \tag{33}$$

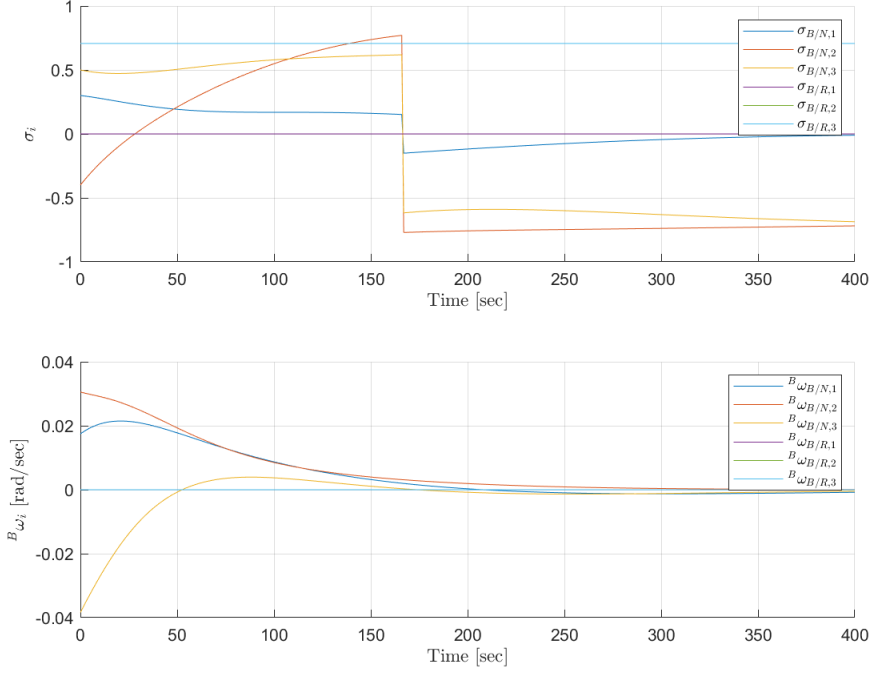
Substituting these gain values back into Eq. (31), we find $T_1 = 120 \text{ s}$, $T_2 = 60 \text{ s}$, $T_3 = 90 \text{ s}$, $\xi_1 = \sqrt{2} \approx 0.7071$, $\xi_2 = 1$, and $\xi_3 = \frac{1}{3}\sqrt{6} \approx 0.8165$, which satisfy the two conditions above.

Over the course of the mission the LMO spacecraft attitude control system must autonomously switch between control modes. All modes use the same PD controller defined in Eqs. (29), (32), & (33), but substitute different frames for the reference frame R . Recall that the LMO spacecraft must Sun-point while sunlit, GMO-point while close to the GMO spacecraft, and nadir point otherwise. We will approximate the LMO orbit eclipse region as the $-\hat{n}_2$ hemisphere in the inertial frame; thus the spacecraft should maintain Sun pointing while ${}^N\vec{r}_{LMO,2} > 0$. We will define "near" the GMO spacecraft as a 35° angle between the positions of the two spacecraft, meaning GMO pointing should be used when in eclipse and $\phi < 35^\circ$. The spacecraft will nadir point when ${}^N\vec{r}_{LMO,2} \leq 0$ and $\phi \geq 35^\circ$. The definitions of the modes are summarized in Table 2.

$$\phi = \cos^{-1} \left(\frac{\vec{r}_{LMO} \cdot \vec{r}_{GMO}}{\|\vec{r}_{LMO}\| \|\vec{r}_{GMO}\|} \right) \tag{34}$$

Table 2: Control Modes

Mode	Ref. Frame	Conditions
Sun Pointing	R_s	${}^N\vec{r}_{LMO,2} > 0$
GMO Pointing	R_c	${}^N\vec{r}_{LMO,2} \leq 0$ & $\phi < 35^\circ$
Nadir Pointing	R_n	${}^N\vec{r}_{LMO,2} \leq 0$ & $\phi \geq 35^\circ$

**Figure 1: Sun Pointing Control Simulation**

XI. Mission Simulations

We began control testing by simulating the system dynamics under each pointing mode individually. Figures 1, 2, and 3 show the performance of the Sun-pointing, GMO-pointing, and nadir-pointing modes respectively. Each simulation used the initial conditions defined in Table 1 and Eq. (2). Note that the attitude and angular velocity responses are asymptotically stable and the 95% settling time approximately matches the $3T = 360$ s settling time that we would expect from the linear approximation in Eq. (30).

Next we simulated the complete mission scenario including autonomous pointing mode switching. This simulation again used the initial conditions from Table 1 and Eq. (2) and ran for a duration of 6500s. The results, shown in Fig. 4, show mode switches at approximately 1917s, 3056s, 4066s, and 5469s, with a ~ 400 s slew following each. Attitude is stable between each transition and, at least qualitatively, tracks the reference attitude well. We can also observe some small overshoots in attitude, matching what we would expect from the damping ratio values of the closed-loop linear system.

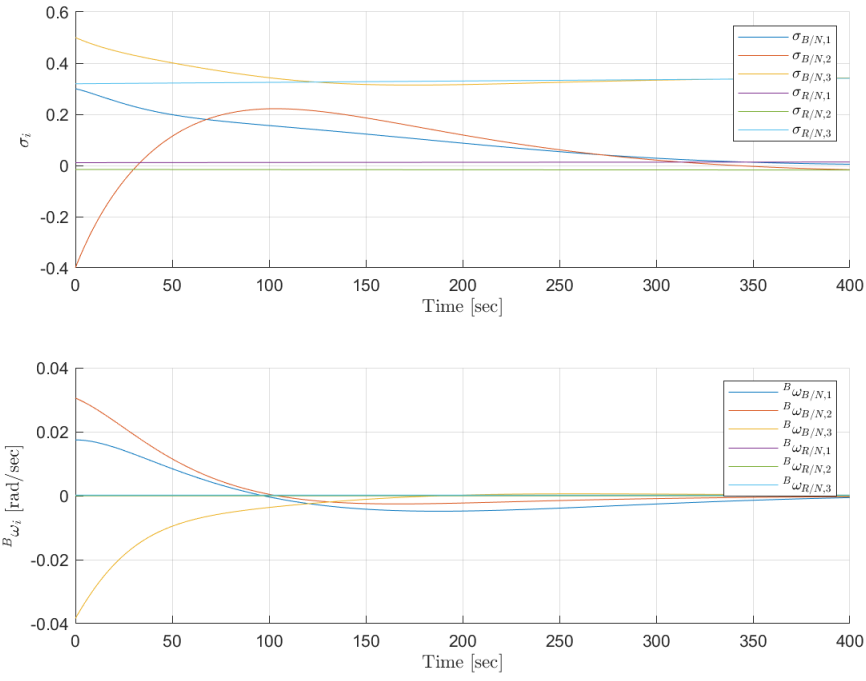


Figure 2: GMO Pointing Control Simulation

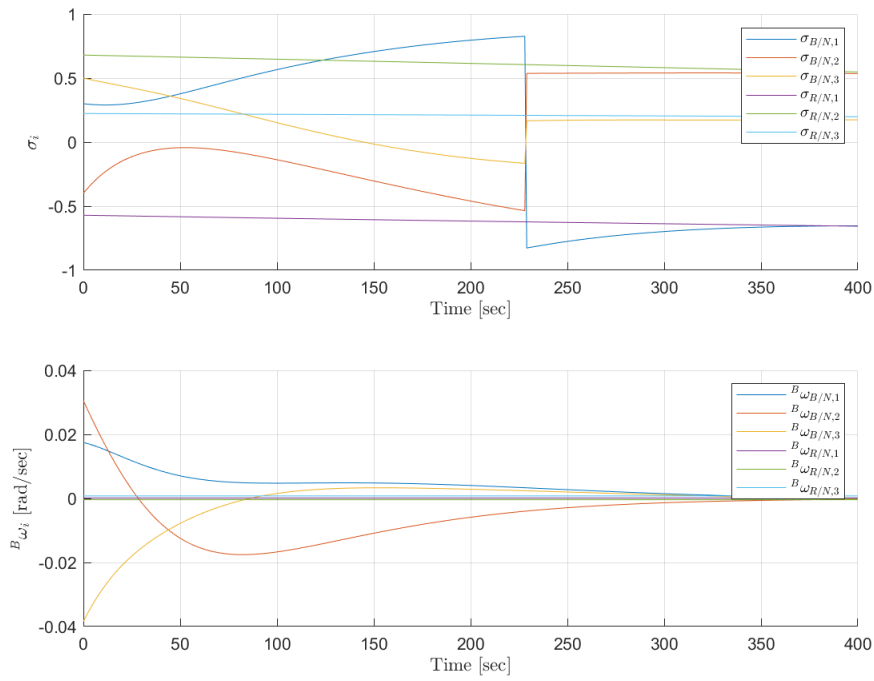


Figure 3: Nadir Pointing Control Simulation

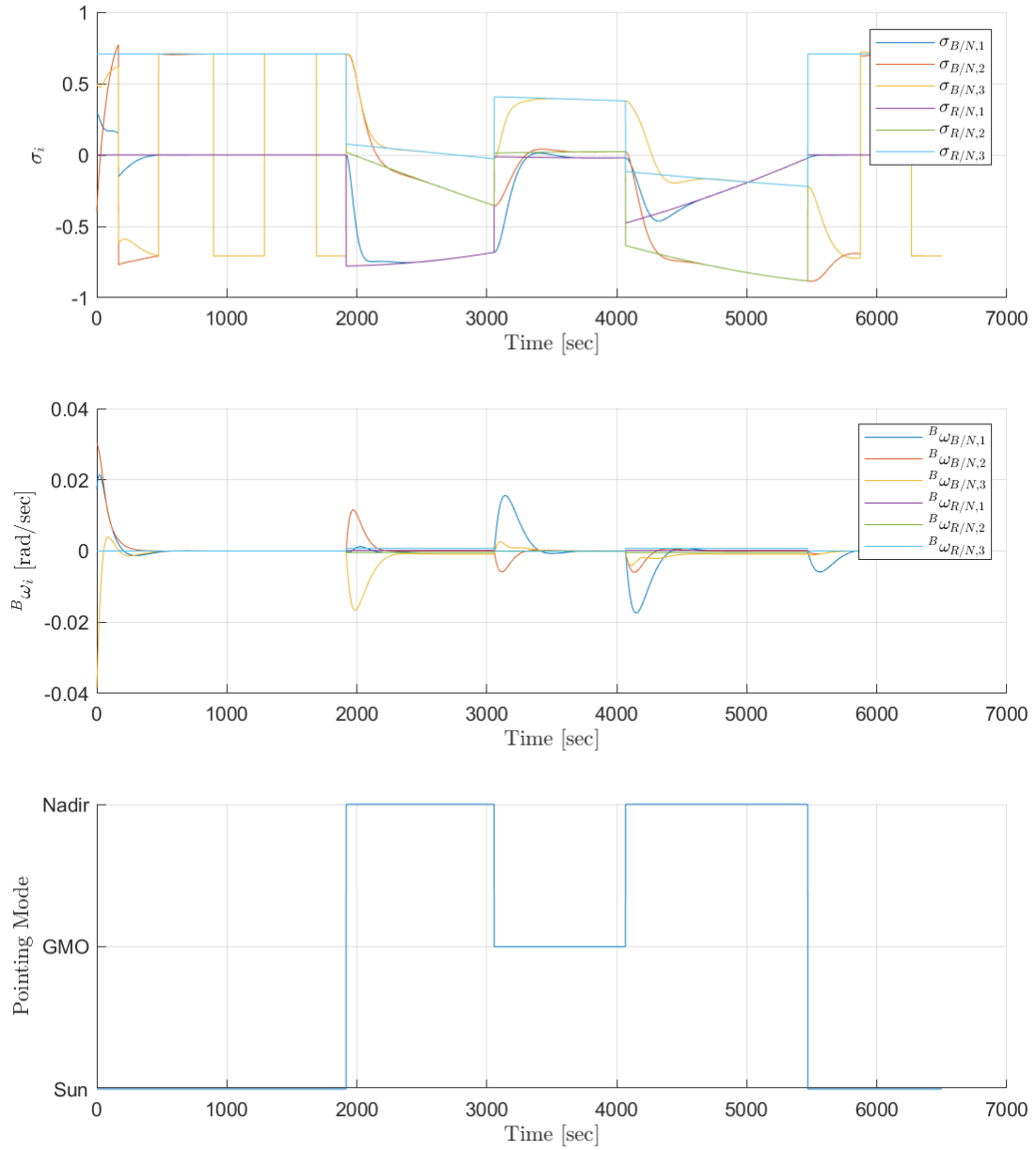


Figure 4: Full Mission Simulation

This attitude dynamics simulation starts from the initial conditions given in Table 1 and Eq. 2 and runs for 6500 seconds. The simulated attitude control system switches between Sun, nadir, and GMO pointing modes based on the simulated circular orbits of the two spacecraft.

XII. Conclusion

In this project we designed and simulated an attitude control system for a nanosatellite in a Mars science mission scenario. Attitude and simple orbital dynamics expressions were derived and simulated numerically. An attitude control law was written and control parameters were tuned based on a linearized system dynamical model. Finally, a set of three pointing control modes was defined, along with logic for autonomous mode switching. The closed-loop spacecraft dynamics were then simulated in each pointing mode, as well as in the full mission scenario. We observed asymptotic stability in each mode and verified the ability of the simulated attitude control system to correctly switch modes autonomously.

References

- ¹Schaub, H. and Junkins, J. L., *Analytical Mechanics of Space Systems*, AIAA Education Series, Reston, VA, 4th ed., 2018.